MULTIGRID PRECONDITIONING OF THE STEAM GENERATOR TWO-PHASE MIXTURE BALANCE EQUATIONS IN THE GENEPI SOFTWARE

Michel Belliard, Marc Grandotto

The 10th International Topical Meeting on Nuclear Reactor Thermal Hydraulics (NURETH-10)
Seoul, Korea, October 5-9, 2003.

MULTIGRID PRECONDITIONING OF THE STEAM GENERATOR TWO-PHASE MIXTURE BALANCE EQUATIONS IN THE GENEPI SOFTWARE

Belliard M., Grandotto M.
CEA-Cadarache, DEN/DTP/STH
Bt 219, F-13108 ST Paul-lez-Durance, France
michel.belliard@cea.fr

KEY WORDS

Two-phase flows, Steam generator, Multigrid, GENEPI

ABSTRACT

In the framework of the two-phase fluid simulations of the steam generators of pressurized water nuclear reactors, we present in this paper a geometric version of a pseudo-Full MultiGrid (pseudo-FMG) Full Approximation Storage (FAS) preconditioning of balance equations in the GENEPI code. In our application, the 3D steady state flow is reached by a transient computation using a semi-implicit fractional step algorithm for the averaged two-phase mixture balance equations (mass, momentum and energy for the secondary flow). Our application, running on workstation clusters, is based on a CEA code-linker and the PVM package. The difficulties to apply the geometric FAS multigrid method to the momentum and mass balance equations are addressed. The use of a sequential pseudo-FMG FAS two-grid method for both energy and mass/momentum balance equations, using dynamic multigrid cycles, leads to perceptibly improvements in the computation convergences. An original parallel red-black pseudo-FMG FAS three-grid algorithm is presented too. The numerical tests (steam generator mock-up simulations) underline the sizable increase in speed of convergence of the computations, essentially for the ones involving a large number of freedom degrees (about 100 thousand cells). The two-phase mixture balance equation residuals are quickly reduced: the reached speed-up stands between 2 and 3 following the number of grids. The effects on the convergence behavior of the numerical parameters are investigated.

1 INTRODUCTION

This paper is devoted to the presentation of the multigrid preconditioning of the mixture momentum balance equations in the CEA GENEPI software (Obry et al., 1990) dedicated to the Steam Generator (SG) simulation. It is based on a geometric pseudo-full multigrid (FMG) version of the Full Approximation Storage method (FAS) to accelerate the solve of the mixture balance equations. The reader can get more details in the reference (Belliard, 2001) and (Belliard, 2003).

The GENEPI code solves the balance equations of an equivalent mixture in a porous media. The following strong formulations of the mixture balance equations are issued from a homogenization process, (Grandotto and Obry, 1996):

1. mass balance

$$\vec{\nabla}.(\beta\vec{G}) = 0 \qquad (1)$$

2. momentum balance

$$\begin{aligned} &\beta\rho\partial_t\vec{v} + \beta\rho(\vec{v}.\vec{\nabla})\vec{v} + div(\beta x(1-x)\rho\vec{v_R}\otimes\vec{v_R}) \\ &= \beta\rho\vec{g} - \beta\bar{\Lambda}\rho\vec{v} - \beta\vec{\nabla}P + div(\beta\mu_T(\vec{\nabla}\vec{v} + \vec{\nabla}^t\vec{v})) \end{aligned} \qquad (2)$$

3. energy balance (enthalpy)

$$\begin{aligned} &\beta\rho\partial_t H + \beta(\vec{G}.\vec{\nabla})H + div(\beta x(1-x)\rho L\vec{v_R}) \\ &= \beta Q + div(\beta\chi_T\vec{\nabla}H) \end{aligned} \qquad (3)$$

Concerning the mixture energy and the mixture momentum balance equations (2) - (3) , the steady-state flow regime is reached by mean of a pseudo-time marching. No time marching is applied for the mixture mass balance equation (1). Hence this approach leads to an algorithm very close to those used in the incompressible fluid dynamic framework: at each pseudo-time step, a Chorin like scheme (Gresho and Chan, 1990) allows the simultaneous computation of the mixture mass flux and the mixture pressure. During a pseudo-time step, the balance equations are successively solved: energy, then momentum/mass balance equations.

Space discretization is done by mean of a Galerkine finite element method (FEM) leading to a weighted integral version of the above equations (weak formulation) in which the mechanical stress term and the energy diffusion one are integrated by part. The unknowns are : H (Q1), P (Q0) and $\vec{v}$ (Q1). The porosity β and the mass flux $\vec{G} = \rho\vec{v}$ are taken in Q1. Generally, the other physical quantities (i.e. ρ, x, μ_T, $\bar{\Lambda}$, ...) are taken in Q0 (i.e. by element). According to the hyperbolic type of the flow equations, Dirichlet boundary conditions are used at the inlets of the domain (mass flux and enthalpy) and Neumann ones at the outlets (pressure). The other boundaries of the domain are adiabatic and impermeable walls. At each pseudo-time step, the arising linear systems are partially solved (5 to 20 iterations) by an iterative method. In order to compute ρ, x and L in function of H and P, we need water thermodynamic tables and the μ_T, χ_T, $\bar{\Lambda}$, $\vec{v_R}$ terms are obtained by the use of a large set of semi-empirical closure relations (Obry et al., 1990). The heat source Q in the enthalpy equation is linked to the resolution of an energy balance equation for the primary flow. To evaluate this term, other correlations on the heat exchange coefficient and the wall temperature are included.

The paper is organized as follow. The Section two is devoted to the presentation of the multigrid correction scheme and of some specific points concerning the FAS correction implementation for the mixture balance equations (energy, momentum and mass). The implementation itself is the object of the Section three. Finally, I present some numerical test cases in the Section four, followed by some concluding remarks.

2 THE FAS METHOD IN THE GENEPI CODE

In the framework of the weighted residual method, a typical problem is to find s ($s \in V$, V is a Hilbert space) solution of :

$$(4) \quad r^I(s) := \int T(s)\phi^I(x)\,dv = 0 \quad \forall \phi^I \in V$$

where $\{\phi^I\}$ is a basis of V, $T(s)$ a residual function of the solution s and $r^I(s)$ the weighted integral of the residual. If u is an approximation of the solution s, the error is defined by $e := s - u$. Roughly speaking, a multigrid technique is an iterative method to solve this equation on a given grid Ω_0 (here, called the finest grid), based on successive estimations of the error on a hierarchy of nested coarser grids Ω_l, $0 < l \leq l_{max}$ where l_{max} is the index of the coarsest grid. It uses a nested sequence of two-grid methods.

In a two-grid method, we perform only some passes of an iterative method on the fine grid Ω_0. Then, on the coarse grid Ω_1, an error equation is formed, involving the restricted fine grid residual $\bar{r}_1 := P_1^0 r_0$ (and the restricted fine grid approximation $\bar{u}_1 := P_1^0 u_0$ in the case of non-linear problems). Then, a coarse grid error is obtained. It is defined by $e_1 := u_1 - \bar{u}_1$. This one is either exact or only estimated. This coarse grid error is then prolonged to the fine grid in order to correct the former estimation of the solution (eventually with a relaxation coefficient α): $u_0 \leftarrow u_0 + \alpha P_0^1 e_1$. This relaxed scheme can be also written as:

$$(5) \quad u_0 \leftarrow (1 - \alpha P_0^1 P_1^0) u_0 + \alpha P_0^1 u_1.$$

In a FAS multigrid method, on each coarse grid Ω_l, $0 < l \leq l_{max}$, the error equation is :

$$(6) \quad \int T_l(u_l)\phi_l^I(x)\,dv = S_l^I \; \forall \phi_l^I \in V_l$$

with :

$$(7) \quad S_l^I := \int T_l(\bar{u}_l)\phi_l^I(x)\,dv + \bar{r}_l$$

There are two ways to construct the coarse grid operators $T_l()$. The first one is to build it only from the fine grid (Ω_{l-1}) equation discretization (arithmetic multigrid version). The second one is based on the discretizations of the balance equations on the coarse grid Ω_l itself (geometric multigrid version). In this paper, we only consider the geometric multigrid version.

Now, we perform some analyses concerning some specific aspects of the introduction of a geometric FAS method for the solving of the mixture balance equations (energy, momentum and mass). They are related to the strong variations of the forcing terms following the space discretization step, to the specific application of the mass flow Dirichlet condition near the walls and the use of the FEM and the Chorin's projection algorithm.

For the full mixture balance equation FAS preconditioning, we restrict the mixture mass flux, pressure and enthalpy, the primary fluid temperature and the mixture momentum and energy balance residuals. As explained here after, the restriction of the mixture mass balance residual is not necessary. Let notice that we choose to restrict the mixture mass flux instead of the mixture velocity for a compatibility reason with the divergence free mass flux constraint. A nodal variable u_{l-1} is restricted by a canonical restriction (in this case, the coarse node I and the fine one i are the same nodes) and a mixture weighted residual by a nodal weighted average restriction. The element variables $u_{l-1}^{e_{l-1}}$ (e.g. mixture pressure) are transferred by mean of an arithmetic average or by a volume weighted restriction. The errors concerning the mixture specific enthalpy, the mass flux, the pressure and the primary fluid temperature must be

computed and prolonged. The prolongation operator used for the nodal quantities is the trilinear interpolation. For the element quantities, we use a direct affectation.

In our geometric version of the FAS multigrid method, the porosity field is independently computed on each grid. We use an unique U-tube bundle description and several computation domain meshes. Consequently, the porosity field β_l and β_{l-1} are different in discontinuity regions (boundaries of the U-tube bundle).

2.1 Divergence Free Mass Flux

The pressure evolution in the Chorin-Gresho algorithm (Gresho and Chan, 1990) is based on successive updates of pressure distributions associated at the divergence free space projections. If we denote $\overrightarrow{G}^* := \rho(H^n, P^n)\overrightarrow{v}^*$ based on the solution $\overrightarrow{v}^*$ of the mixture momentum balance equation (2) using the pressure value taken at the previous pseudo-time step P^n, we have:

$$\overrightarrow{G}^{i,n+1} = \overrightarrow{G}^{i,*} - \frac{\sum_e \int \lambda^e \overrightarrow{\nabla}(\beta\phi^i)\, dv}{\int \beta\phi^i\, dv} \quad (8)$$

and

$$P^{e,n+1} = P^{e,n} - \frac{2\lambda^e}{\delta t} \quad (9)$$

with λ^e solution of a weak formulation of the following equation:

$$\overrightarrow{\nabla}.\beta\overrightarrow{\nabla}\lambda = \overrightarrow{\nabla}.\beta\overrightarrow{G}^*. \quad (10)$$

This scheme is also used to satisfied the free divergence constraint for a given mass flux field. For each pseudo-time step, the divergence free constraint equation (1) is solved to the computer precision. Hence, the term $\bar{r} = P_l^{l-1} r_{l-1}$ in Equation (7) is zero. But, the mass flow restricted on the coarse grid $\overrightarrow{G_l}$ is not generally divergence free. Hence, the coarse grid FAS corrected mass balance equation is no longer compatible with the the coarse grid mass flow divergence free condition. So, the pressure Poisson equation (10) must be adapted. For the strong formulation of the balance equations, it becomes:

$$\overrightarrow{\nabla}.\beta_l\overrightarrow{\nabla}\lambda_l = \overrightarrow{\nabla}.\beta_l\overrightarrow{G_l}^* - \overrightarrow{\nabla}.\beta_l\overrightarrow{G_l}. \quad (11)$$

2.2 Boundary Conditions

Usualy, the user specifies the mixture mass flow rate Q_{in} and the mixture specific enthalpy H_{in} at the inlets and the pressure is specified P_{out} at the outlet. Concerning the outlet pressure and the inlet enthalpy, the locations and the values of the boundary conditions are similar for all the grids. It is not longer true for the inlet mass fluxes, since similar mass flow rates for all the grids lead to different inlet average mixture velocities (the inlet porosities may change). For each pseudo-time step, using the mixture density distribution $\rho(H_{in}, P)$, new inlet mixture velocity values are deduced:

$$\overrightarrow{v}_{in} = \frac{Q_{in}}{\rho \int_{S_{inlet}} \beta dS \overrightarrow{n}}. \quad (12)$$

and assigned to the inlet nodes. To avoid discrepancies in the boundary conditions between the several grids, the values of the fine grid inlet mass fluxes are restricted on the coarse grid inlet nodes.

2.3 Pressure Computation

As previously mentioned, the pressure evolution in the Chorin-Gresho algorithm is based on successive updates of the initial pressure distribution. This initial pressure must be in coherence with the initial mass flux (Consistent Pressure Poison Equation -CPPE- solver). Then, a pressure update is performed at each divergence free space projection. In the case of the FAS algorithm, two error terms are potentially prolonged on the fine grid: the mass flux error and the pressure error. Simultaneously applying these two error corrections breaks the coherence between the velocity and the pressure. Indeed, we apply the mass flux error correction and then compute a new fine grid pressure field solving the CPPE, before running the Picard iterations.

2.4 Forcing Terms

As previously mentioned, the porosity fields may be different on each grid: the β_l field is build by intersecting several meshes of the inner technological devices (U-tube bundle, baffles, ...) with the computation domain mesh Ω_l. Consequently, following the geometrical scale addressed, the forcing terms may be strongly different. For example, friction forces may be apply to a coarse grid node, but not to the equivalent fine grid node, see Fig. 1. Friction forces are induced by the U-tube bundle or the baffles included in the cells. Hence nodal friction forces are spread on the whole nodes belonging to cells "with friction forces" (see Fig. 1).

The forcing term formulation on a given grid has no direct relation with the formulations on the other grids (geometrical multigrid version). Hence, the coherence of the several formulations between the grids is not generally assumed. Clearly, this point may limit the error reduction in the multigrid algorithm as seen in the FAS correction of the mixture energy balance equation (Belliard, 2001).

2.5 Primary Fluid Energy Balance Equation

We don't implement the FAS method for the the primary fluid energy balance equation. This equation is very easily and quickly solved on the primary curvilinear grid. However, because it is implied in the source term in the RHS of the mixture energy balance equation, we compute a coarse grid restriction and a coarse grid error of the primary fluid temperature. A fine grid correction is then performed.

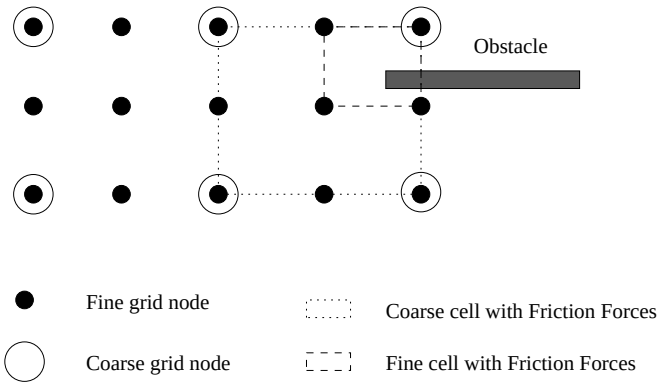

Figure 1: Forcing Terms

3 AN IMPLEMENTATION

In this Section, we review the expressions of the coarse grid correction terms (term S_l^I of Equation (6)) for the energy balance equation, the momentum balance equation and the mass balance equation, the definition of the error criterion driving the dynamic multigrid cycle and we present our FAS algorithm.

We can do a remark. Multigrid method are first of all useful in case of a big number of cells. To day, a computation involving 250,000 cells needs about 1 Gigabytes memory and three grids is enough even for this reference computation. In fact, with hexahedral elements in 3-D geometry, the coarsening ratio between two consecutive grids is 8 and, for a four level multigrid algorithm, the cell number ratio between the finest and the coarsest grid is $8^4 = 4096$. Hence, the coarsest grid for our reference computation contains only about 60 cells. It is too small for an efficient simulation.

3.1 Coarse Grid Correction Terms

We have to compute the S_l^I term of Equ. (6) . It is formed by two parts. The first one is the $\int T_l(\bar{X}_l)\phi_l^I(x)\,dv$ term built using the restricted variables $\bar{X}$ (see below). The second one is completely defined by the chosen restriction (nodal weighted average restriction for the nodal residuals). It is worth to notice that the first part of the correction terms are the coarse grid non-linear residuals of the fully non-linear steady-state flow balance equations, built with the restrictions of the primary fluid and mixture variables. The values of the coefficients implied in the coarse grid correction terms (denoted *restricted* coefficients) are evaluated using these restricted variables. The *restricted* coefficients are: $\bar{\chi}$, $\bar{L}_l$, $\bar{\rho}_l$, $\bar{\mu}$, $\bar{\chi}_T$, $\bar{\bar{\Lambda}}_l$, $\bar{\vec{k}}_l$.

3.1.1 Energy Balance Equation

The term $\int T_l(\bar{X}_l)\phi_l^I(x)\,dv$ is computed by (subscript l stands the coarse grid) :

$$\begin{aligned}\int T_l(\bar{X}_l)\phi_l^I(x)\,dv \equiv & \int dv\,\phi_l^I(x)[\beta_l(\vec{\bar{G}_l}.\vec{\nabla})\bar{H}_l + div(\beta_l\,\bar{\chi}(1-\bar{\chi})\bar{\rho}_l\bar{L}_l\,\vec{\bar{k}}_l)] \\ & - \int dv\,\phi_l^I(x)\beta_l\bar{Q}_l + \int dv\,\vec{\nabla}\phi_l^I(x)(\beta_l\bar{\chi}_T\vec{\nabla}\bar{H}_l)\end{aligned} \tag{13}$$

with the *restricted* coefficients defined as previously mentioned and $\bar{Q}_l$ the *restricted* source term, including the *restricted* volume thermal source computed with the restricted primary fluid temperature, the coarse grid boundary thermal flux and, eventually, the *restricted* pressure gradient terms (if it exists, this last term is a function of the restricted variables).

3.1.2 Momentum Balance Equation

For the momentum balance equation, the term $\int T_l(\bar{X}_l)\phi_l^I(x)\,dv$ is computed by :

$$\begin{aligned}\int T_l(\bar{X}_l)\phi_l^I(x)\,dv \equiv & \int dv\,\phi_l^I(x)[\beta_l\bar{\rho}_l(\vec{\bar{\gamma}}.\vec{\nabla})\vec{\bar{\gamma}} + div(\beta_l\,\bar{\chi}(1-\bar{\chi})\bar{\rho}_l\,\vec{\bar{k}}_l\otimes\vec{\bar{k}}_l)] \\ & - \int dv\,\phi_l^I(x)\beta_l\bar{\rho}_l(\vec{g} - \bar{\bar{\Lambda}}_l\vec{\bar{\gamma}}) - \int dv\,\vec{\nabla}\phi_l^I(x)[\beta_l\bar{P}_l - \beta_l\,\bar{\mu}(\vec{\nabla}\vec{\bar{\gamma}} + \vec{\nabla}^t\vec{\bar{\gamma}})] + BC\end{aligned} \tag{14}$$

3.1.3 Mass Balance Equation

The term : $\int T_l(\bar{X}_l)\psi_l^E(x)\,dv$ (a correction field by element) is computed by ($E := e_l$) :

$$\int T_l(\bar{X}_l)\psi_l^E(x)\,dv \equiv \int dv\,\psi_l^E(x)\,\vec{\nabla}.(\beta_l\vec{G}_l). \tag{15}$$

In fact, we don't solve directly this equation, but we enforce the divergence free projection of the gap mass flux: $(\overrightarrow{G_l} - \overrightarrow{\overline{G_l}})$.

3.2 A Criterion To Stop The Dynamic Multigrid Cycle

An important feature is related to the going out of the multigrid cycles. In fact, the high efficiency of the multigrid solver is drastically reduced after some cycles, leading to a stalled regime in case of static cycle. To overcome this drawback, we need an *ad hoc* test on the relative variations of the errors (testing if the error no longer decreases). Doing this, we face to dynamic multigrid cycles. The goal is to stop the coarse grid runs (or reduce the associated computational cost) and to disconnect the corrections of the variables for the fine grid. The first point is motivated by the high cost of the computation in regard of the communication one.

For the mixture specific enthalpy and the mixture mass flux, we build the following indicator set (Ω_l, $l = 1, ... \ l_{max}$):

$$ind_l(e_l) = \frac{abs(|e_l|^m_{L2} - |e_l|^{m-1}_{L2})}{|e_l|^{ref}_{L2})} \quad (16)$$

where e_l is the coarse grid error, m is the multigrid cycle counter, $||_{L2}$ denotes the discrete L_2-norm, $|e_l|^{ref}_{L2}$ a reference L_2-norm (here, $|e_l|^1_{L2}$) and abs(...) the absolute value function. Doing this, the corrections on the finer grid Ω_{l-1} is monitored by the stalled regime detections of the computed errors itself.

For each coarse grid task, we can give a general tolerance level ε^{MG}_l. The default value for the industrial SG simulations is $5 * 10^{-3}$ but it can be user managed. If during the computation, we reach the following condition for one of the coarse grid error (specific enthalpy error or mass flux error):

$$ind_l(e_l) < \varepsilon^{MG}_l, \quad (17)$$

the value of the computed error is bring to zero. When, this condition is reached for the specific enthalpy and the mass flux, the value of the coupling period for the task related to the grid M_l is gradually reduced to two iterations (we successively multiply by 0.8 the coupling period).

3.3 The Two-grid Algorithm

A GENEPI two-grid cycle is a pseudo-FMG FAS two-grid slash-cycle (without post-smoothing) since no correction is applied during the first cycle. Hence, the effective computation begins by a coarse grid solving. The number of coarse grid pseudo-time steps involved in the first cycle cp^0_l is user managed. If this number is big enough (of the same magnitude that the pseudo-time step number required to solve the coarse grid problem alone), we get a *true* FMG method. If it is only equal to the current number of pseudo-time steps cp_1, then we get a pseudo-FMG method.

3.4 A Red-black Parallel Version Of A Three-grid Algorithm

A two-grid FAS Method is essentially a sequential method. We have tested a parallel red-black three-grid method. As in a red-black Jacobi method, two groups of grids are set-up (here : $\{M_0, M_2\}$ and $\{M_1\}$). The two groups work sequentially and all the tasks of the same group work in parallel. The groups are set-up in the way that two consecutive grids do not belong to the same group. Following this rule, we apply a sequential non-ideal two-grid method to each couple of consecutive grids. See Belliard (2001) for more details.

4 NUMERICAL TESTS

To test our implementation of the FAS method on steam generator two-phase fluid simulations, we present some sequential two-grid and parallel red-black three-grid computations of the CEA Clotaire mock-up (Campan and Bouchter, 1988). The riser part forms a half cylinder of 0.62 m in diameter and 9.16 m in height. The inside is filled with U-shaped tube bundle, 7.2 m in height, into which the hot primary flow enters. One flow distribution baffle, nine tube support plates and one anti-vibration bar are fixed in respectively the bottom, upright and curved part of the bundle. The simulation fluid is Freon (r114).
Except when it is mentioned, the boundary conditions, the physical and numerical parameters are identical for all the computations. We stop the computation when each variable u (specific enthalpy, mass flux, pressure, primary fluid temperature) has verified a steady-state flow criterion *crit*:

$$\frac{|u^{n+1}-u^n|_{L2}}{|u^n|_{L2}\delta t} \leq crit. \quad (18)$$

with $crit = 10^{-3}s^{-1}$ or $10^{-4}s^{-1}$. These computations differ by the number of grids (2 or 3), the number of fine grid cells (22,400 or 88,704), the *smoother* type (CG or CGS), the pseudo-time step number during the first multigrid cycle (cp_l^0, $0 < l \leq l_{max}$), the coupling periods cp_l and the dynamic multigrid cycle cut-off criteria ε_l^{MG} (see Equation 16).

Our reference computation is a pseudo-FMG FAS simulation involving the following numerical parameters:

- $cp_0 = 15$, $cp_1 = 60$ and $cp_2 = 120$,
- preconditioned CG smoother,
- $\alpha = 0.7$, $\varepsilon_1^{MG} = 10^{-3}$ and $\varepsilon_2^{MG} = 10^{-3}$ (dynamic multigrid cycle cut-off criteria on the coarse grids).

Each fine grid is built by subdivision of the coarser one: each coarse grid cell is cut in eight parts. The 22,400 cells fine grid is shown on Figures 2 and 3 with its associated coarse grid (2,800 cells). Computations involving 22,400 grid cells are run on a 1,700 MHz PIV Personal Computer (roughly one hour CPU time and 100 Mb). Computations involving 88,704 grid cells are run on the CEA supercomputer IXIA, a 64 Dec-Alpha ES40 stations with four 833 MHz EV68 processors (roughly height hours CPU time and 700 Mb). Results are compared in terms of pseudo-time step number and CPU time (eventually, elapsed time).

4.1 Clotaire Mock-up Sequential Two-grid FAS Simulations

4.1.1 The 22,400-cell Grid

Table 1 shows the reference computation results in comparison with the standard computation and the FMG FAS method ones. Concerning the fine grid, Figure 4 shows the convergence histories of the mixture flow variables and Figure 5 shows the evolutions of the corrections of these variables u ($\frac{|u^{new}-u^{old}|}{|u^{old}|_{L2}}$), and of the non-linear balance equation residuals in relative discrete L^2 norm. The CPU time speed-up is 1.5 for the reference computation. As a whole, the coarse grid solution does bring an acceleration of the fine grid computation: about 57% of the standard computation fine grid pseudo-time steps are saved (the iteration speed-up is about 1.7). The dynamic multigrid cycles are stopped before the obtention of the 10^{-3} s^{-1} steady-state criteria and after this point the standard method is run. The number of multigrid cycles is 25 ($\equiv$ 15*25 = 375 fine grid pseudo-time steps or 1500 coarse grid pseudo-time

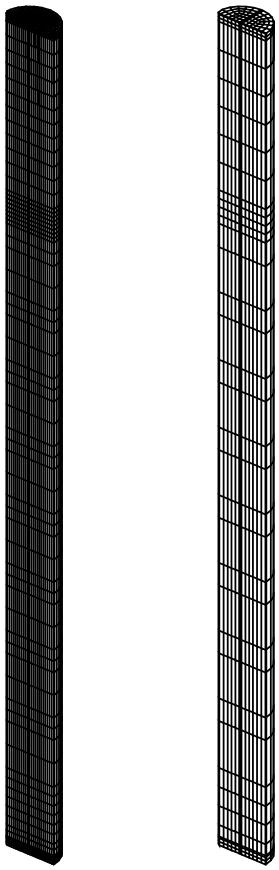

Figure 2: Fine (22,400 cells) and coarse grid (2,800 cells).

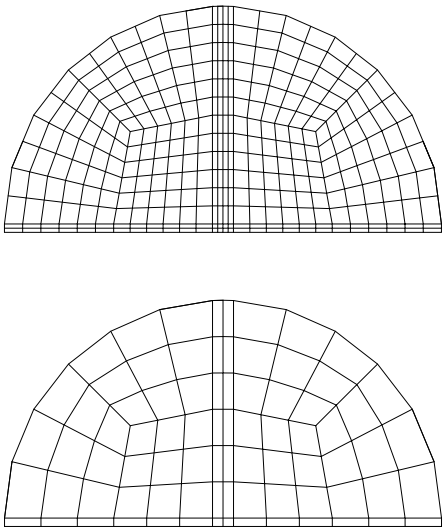

Figure 3: Fine (22,400 cells) and coarse grid (2,800 cells): cross-sections.

steps).

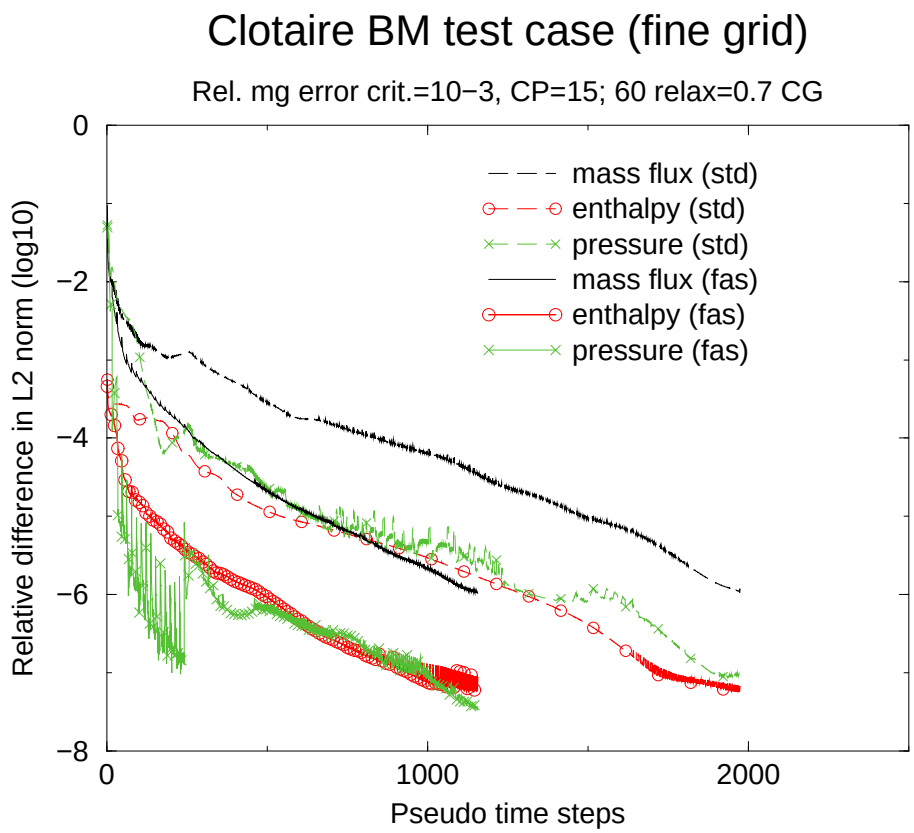

Figure 4: Clotaire mock-up simulations: comparison of the convergence histories of the fine grid variables for the FAS method and the standard solver in L^2 norm. Pseudo-FMG FAS method: 22,400 cells, $cp_0 = 15$, $cp_1 = 60$, $\varepsilon_1^{MG} = 10^{-3}$, $\alpha = 0.7$; CG smoother.

The true application of the FMG algorithm does not increase the CPU time speed-up: the number of fine grid pseudo-time steps roughly is the same as for the pseudo-FMG FAS computation and the first 900 coarse grid pseudo-time steps lead to a CPU time overhead without compensation, see Table 1.

An important feature is the fine grid correction of the primary flow temperature. It provides a substantial increase in the mixture enthalpy convergence. Without correction, the specific enthalpy conver-

Table 1: Clotaire mock-up simulations (steady-state: 10^{-3} s^{-1}); sequential two-grid FAS method: 22,400 cells, $cp_0 = 15$, $cp_1 = 60$ (first $cp_1 = 900$; FMG FAS) $\alpha = 0.7$, $\varepsilon_1^{MG} = 10^{-3}$, CG smoother.

	Std	Pseudo-FMG FAS		FMG FAS	
	Ω_0	Ω_1	Ω_0	Ω_1	Ω_0
Steady-state ($10^{-3}s^{-1}$):					
Pseudo-time step counter	1,472	1,782	630	2,566	645
PIII CPU time(s)		*1,315.7*		*1,795.2*	
PIV CPU time (s)	3,478.6		1,625.1		1,664.8
Speed-Up (CPU time)			**1.5**		**1.5**
Speed-Up (iterat.)			**1.7**		**1.4**

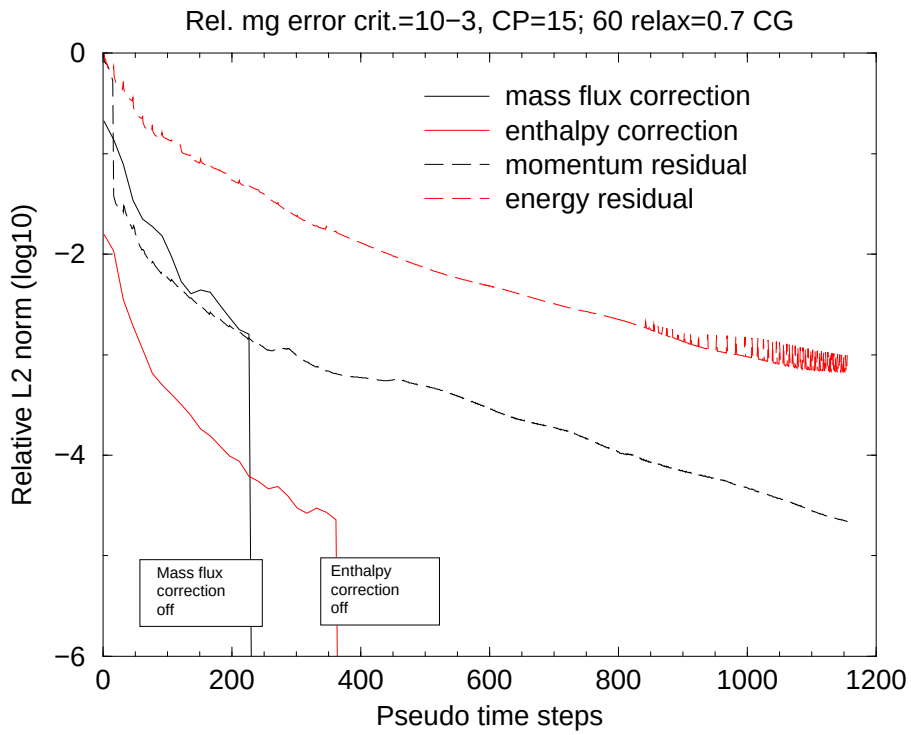

Figure 5: Clotaire mock-up simulations: convergence histories of the fine grid variable corrections ($\alpha P_0^1 e_1$) and non-linear residuals in L^2 norm. Pseudo-FMG FAS method: 22,400 cells, $cp_0 = 15$, $cp_1 = 60$, $\varepsilon_1^{MG} = 10^{-3}$, $\alpha = 0.7$; CG smoother.

gence is not so fast, due to the coupling of the mixture energy balance equation with the primary fluid one and the physical time needed to propagate the primary flow information.

As a whole, the speed-up bring by the pseudo-FMG FAS method is similar to the nested iteration method one for this degres of freedom number. In this very much simpler method, we only use a coarse gird computation result to initialize the fine grid computation. In fact, the 88,7040-cell grid test case will show the advantage of the pseudo-FMG FAS method in the case of a big degres of freedom number.

4.1.2 The 88,7040-cell Grid

Again, the reference computation is confronted to the standard method computation. We give the CPU time and the elapsed time, more representative of the performances seen by the user. For the standard method computation the CPU time and the elapsed one are similar (no communication time). For the FAS methods, speed-up measurements based on the elapsed time lead to low bound values of the CPU time speed-up.

Table 2 gives a comparison between the results and the Figure 6 shows the convergences of the fine grid variables. For this high space resolution computation, the pseudo-FAS method performance is higher than the nested iteration method one (speed-up values about 2.0). As a whole, the FAS algorithm performance is very good, even larger than in the case of the 22,400-cell grid: about 2.5 instead of 1.5. Explanation is to be found in a relative cheaper coarse grid pseudo-time step cost and a lower efficiency of the standard method in term of convergence: 3,887 instead of 1,472 fine grid pseudo-time steps. After 25 multigrid cycles ($\equiv$ 375 fine grid pseudo-time steps), the dynamic multigrid cycle cut-off criterion

Table 2: Clotaire mock-up simulations (steady-state: $10^{-3}\ s^{-1}$); sequential two-grid pseudo-FMG FAS method: 88,704 cells, $cp_0 = 15$, $cp_1 = 60$, $\alpha = 0.7$, $\varepsilon_1^{MG} = 10^{-3}$, CG smoother.

	Standard	Pseudo-FMG FAS	
	Ω_0	Ω_1	Ω_0
Pseudo-time step counter	3,887	2,435	1,170
Elapsed time (s)	29,366.3		12,001.0
CPU time (s)	29,330.5	2,340.1	9,198.6
Memory (Mbyte)	696.2	75.9	709.5
Speed-Up (elaps. time)			**2.4**
Speed-Up (CPU time)			**2.5**
Speed-Up (pseudo-time steps)			**2.7**

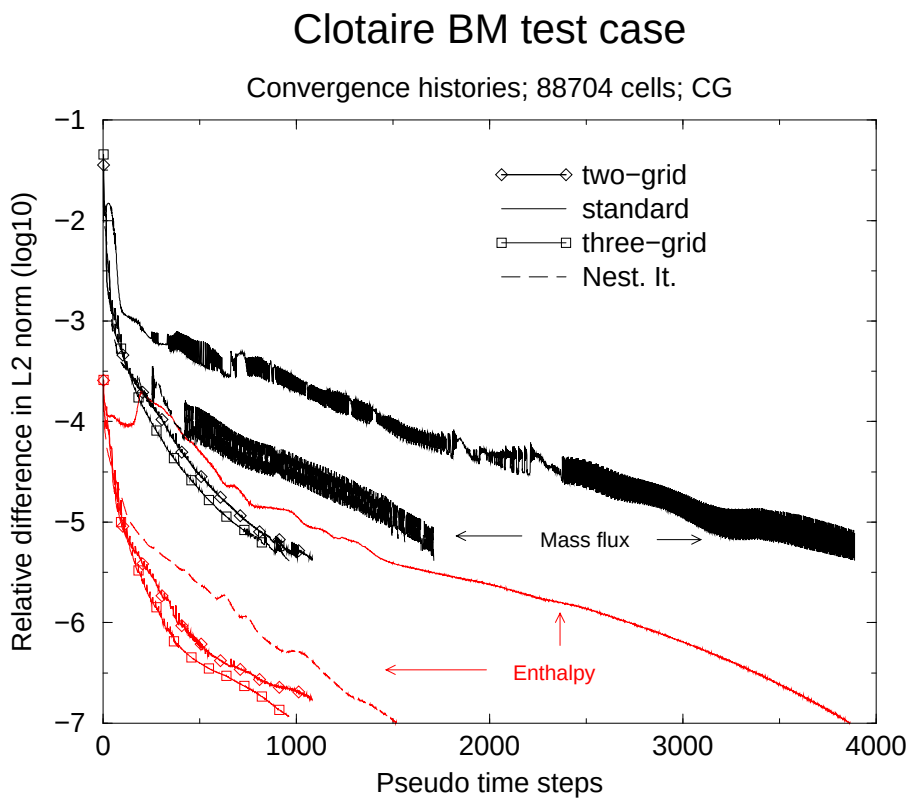

Figure 6: Clotaire mock-up simulations: comparison of the convergence histories of the fine grid mass flux and pressure for the FAS method, the nested iteration method and the standard solver in L^2 norm. Pseudo-FMG FAS methods: 88,704 cells, $cp_0 = 15$, $cp_1 = 60$, $cp_2 = 120$, $\varepsilon_1^{MG} = 10^{-3}$, $\varepsilon_2^{MG} = 10^{-3}$, $\alpha = 0.7$; CG smoother.

($\varepsilon_1^{MG} = 10^{-3}$) is reached for the mass flux. And after 35 multigrid cycles ($\equiv$ 525 fine grid pseudo-time steps), the dynamic multigrid cycle cut-off criterion is reached for the specific enthalpy. Then, the FAS method is stopped and the standard one is run. The slope change of the specific enthalpy convergence at this time is related to this solver change, see Figure 6.

Using a higher value of the ε_1^{MG} criterion leads to reduce the number of fine grid pseudo-time steps. With $\varepsilon_1^{MG} = 10^{-4}$, 50 multigrid cycles are performed and the fine grid pseudo-time step number is reduced to 1,080 (instead of 1,170). But the increase of the coarse grid pseudo-time step number limits the increase of the speed-up.

4.2 Clotaire Mock-up Parallel Red-black Three-grid Pseudo-FMG FAS Simulations

The simulation of the Clotaire mock-up using the 88,704-cell grid is now performed with the parallel red-black three-grid pseudo-FMG FAS algorithm introduced above. The computation parameters are similar to the Section 4.1.2 ones. We confront our reference computation with the sequential two-grid pseudo-FMG FAS method computation of Section 4.1.2.

Table 3 shows the reference computation results. Comparison with the Table 2 points out a fine grid pseudo-time step number reduction: 1,005 instead of 1,170, and an other one for the intermediate grid pseudo-time steps: 1,773 instead of 2,435. This enhanced convergence is summarized in the pseudo-time step number speed-up: 3.1 instead of 2.7 for the sequential two-grid pseudo-FMG FAS method computation. Moreover, taking advantage of a parallel run (Ω_0 in parallel with Ω_2) and of the Ω_1 pseudo-time step number reduction, the elapsed time speed-up is close to the pseudo-time step speed-up (or the CPU time speed-up).

Table 3: Clotaire mock-up simulation (steady-state: $10^{-3}\ s^{-1}$); parallel red-black three-grid pseudo-FMG FAS method: 88,704 cells, $cp_0 = 15$, $cp_1 = 60$ $cp_2 = 120$, $\alpha = 0.7$, $\varepsilon_1^{MG} = 10^{-3}$, $\varepsilon_2^{MG} = 10^{-3}$, CG smoother.

	Standard	Pseudo-FMG FAS		
	Ω_0	Ω_2	Ω_1	Ω_0
Pseudo-time step counter	3,887	2,202	1,773	1,005
Elapsed time (s)	29,366.3			9,714.5
CPU time (s)	2,9330.5	510.3	1,752.0	7,800.3
Memory (Mbyte)	696.2	10.1	76.2	709.5
Speed-Up (Elaps. time)				**3.0**
Speed-Up (CPU time)				**3.1**
Speed-Up (pseudo-time steps)				**3.1**

Concerning the dynamic multigrid cycle algorithm, the cut-off criterion ($\varepsilon_1^{MG} = 10^{-3}$) is reached for the mass flux after 23 multigrid cycles and after 25 multigrid cycles for the specific enthalpy (more quickly than for the two-grid pseudo-FMG FAS case).

4.3 Choice Of The Fine Grid Correction Relaxation

Relaxation is a crucial point for the Clotaire mock-up simulation with the FAS method. Figure 7 shows the influence of the choice of the relaxation parameter α for computations involving the 22,400-cell grid (two-grid method). We look at the mixture mass flux convergence because generally it is the variable that has the slowest convergence. Clearly, choosing α in the range [0.4; 0.9] leads to similar mass flux convergence histories (even if [0.7; 0.9] seems the best interval). Using a value of 1 (*i. e.* no relaxation) induces the divergence of the pseudo-FMG FAS method.

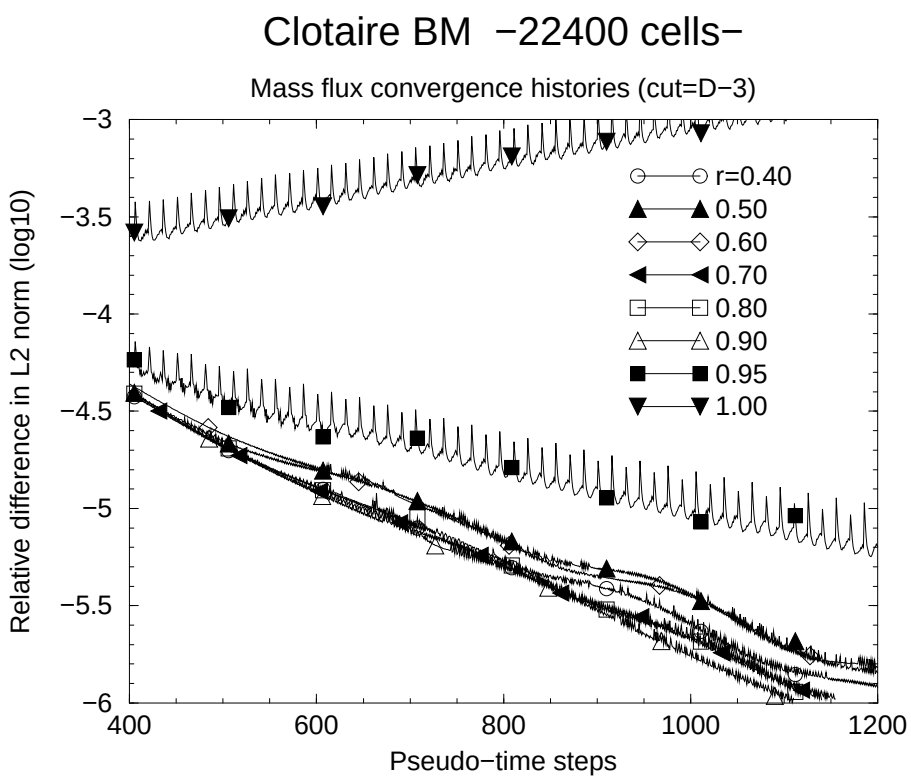

Figure 7: Clotaire mock-up simulations: comparison of the convergence histories of the fine grid mass flux (L^2 norm) function of the relaxation parameter α. Pseudo-FMG FAS method: 22,400 cells, $cp_0 = 15$, $cp_1 = 60$, $\varepsilon_1^{MG} = 10^{-3}$; CG smoother.

4.4 Choice Of The Coupling Periods

Figure 8 shows the influence of the choice of the coupling periods for computations involving the 22,400-cell grid (two-grid method). The dynamic multigrid cycle cut-off criterion is fixed to 10^{-5}. This very low value allows to catch all the convergence behaviors induced by the multigrid corrections. Let us notice that the stalled regime is reached after about 1,000 fine grid pseudo-time steps (except for the (15; 60) computation, and after this point, a standard method is run.

As a whole, all the convergence histories are spread near the coarse grid standard method convergence history. But, particular choices of the coupling periods bring the best convergences. It is the case of the couple (15; 60) (understand $cp_0 = 15$ and $cp_1 = 60$). Moreover, some similarities in the convergence histories can be found. For instance, (15; 30) and (30; 60) lead to the same convergence. For these two couples, the coarse grid / fine grid ratio is the same. Similar convergence properties can also be found for the couples (15; 60) and (15; 120). This last point underlines that 60 coarse grid pseudo-time steps is enough to *solve* the coarse grid problem. At the opposite, if the two coupling periods are too close each other, as (20; 20) or (15; 30), the coarse grid problem is not *solve* with enough accuracy, leading to a slower convergence on the fine grid.

4.5 Pseudo-FMG FAS Method Scalability

We can define the scalability as the following. Suppose a problem involving *nd* degrees of freedom solves in *nt* pseudo-time steps with a multigrid method using a given number of 3D grids. If we multiply *nd* by height and use one additional grid, then the number of pseudo-time steps should be *nt* again.

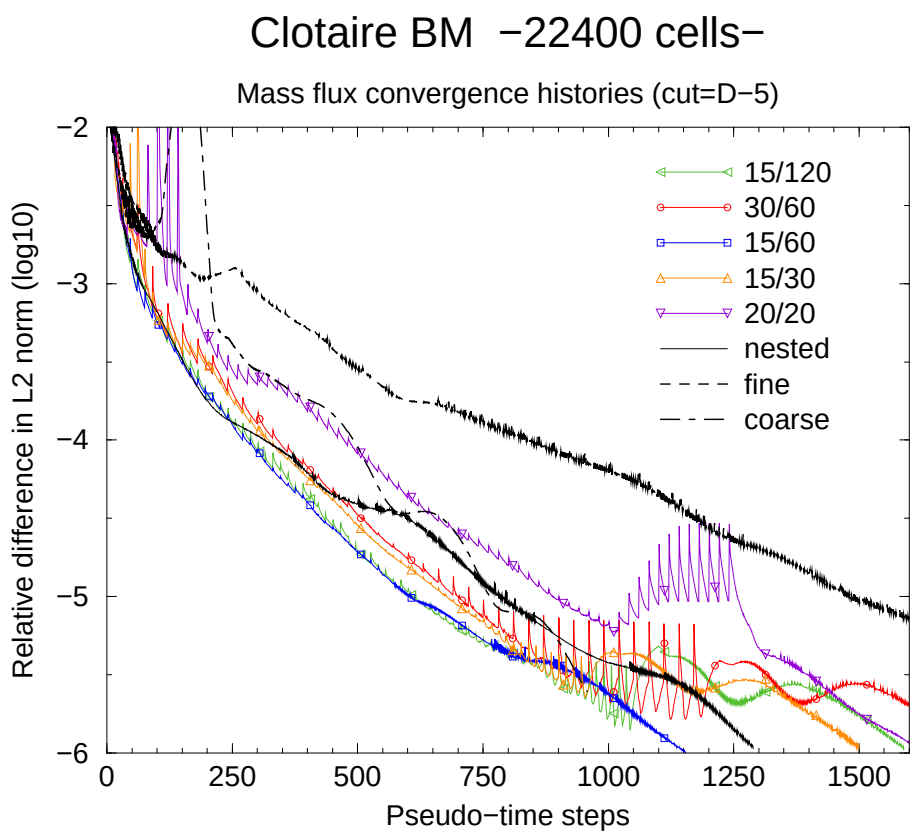

Figure 8: Clotaire mock-up simulations: comparison of the convergence histories of the fine grid mass flux (L^2 norm) function of the coupling periods cp_l. Pseudo-FMG FAS method: 22,400 cells, $\varepsilon_1^{MG} = 10^{-5}$, $\alpha = 0.7$; CG smoother.

Figure 9 shows the comparison of fine grid mass flux convergences for 88,704 cells (three grids), 22,400 cells (two grids) and 2,800 cells (one grid; 22,400/8 cells). Also it shows the convergences related to the one-grid standard method for 88,704 cells, 22,400 cells and 11,088 cells (88,704/8). During the first 500 pseudo-time steps (active multigrid solver), it indicates a pretty nice scalability of the pseudo-FMG FAS method. The cell number ratio between 88,704 and 22,400 is only about four and not eight, but standard method computations show similar mass flux convergence behaviors for the 22,400-cell grid and the 11,088-cell grid test cases (about the same space dicretization following the mean flow direction) that suggests roughly similar convergences for the 11,088-cell and 22,400-cell two-grid pseudo-FMG FAS method.

5 CONCLUDING REMARKS

The FAS multigrid method has been successfully implemented and tested in the GENEPI code. The high efficiency of this scheme as been proved in the case of an industrial simulation as the Clotaire Benchmark one. The FAS algorithm performances are very good, but need a large amount of computational cells to really be efficient. For a 22,400-cell test case, the CPU time speed-up is relatively low: roughly 1.5 (two grids). But for the 88,704-cell test case, high CPU time speed-up is obtained: about 2.5 (two grids) and 3.0 (three grids). Larger is the number of grid cells (here, one hundred thousand), bigger is the speed-up.

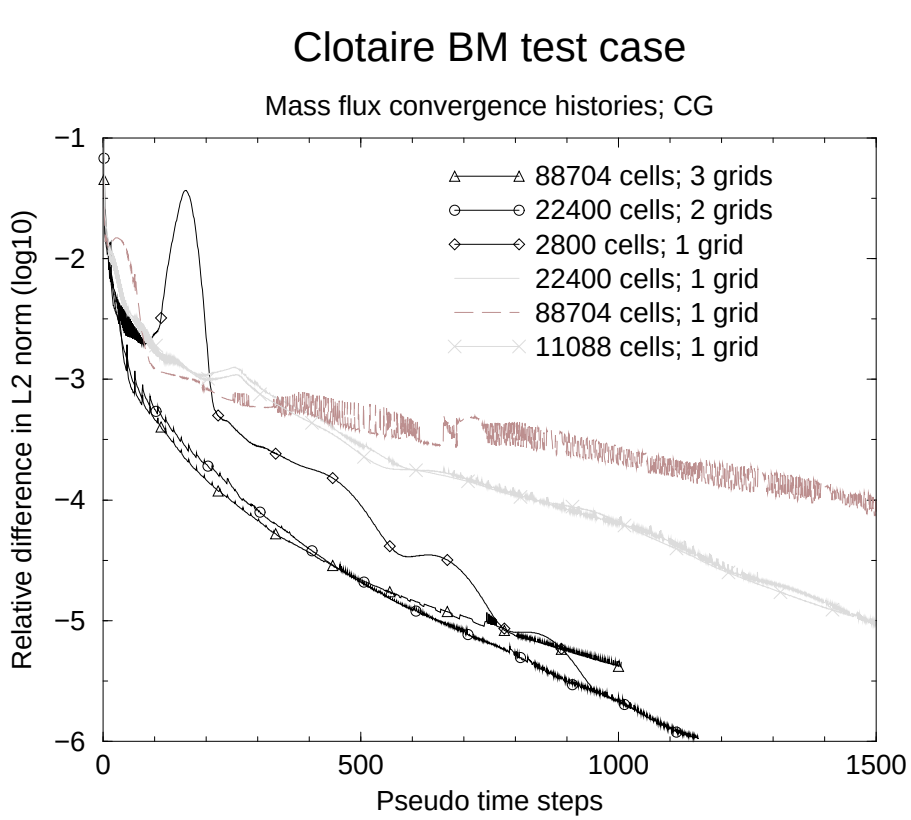

Figure 9: Clotaire mock-up simulations: comparison of the convergence histories of the fine grid mass flux (L^2 norm). Pseudo-FMG FAS method: $cp_0 = 15$, $cp_1 = 60$, $cp_2 = 1,200$, $\alpha = 0.7$, $\varepsilon_1^{MG} = 10^{-3}$; CG smoother. Scalability test.

Moreover, parameter studies has been performed providing the determination of a set of parameter values leading to the best results. In term of CPU time, the true version of the FMG method is not the best one to maximize the speed-up. Pseudo-FMG algorithms reach a better score. The relaxation of the fine grid error correction and a dynamic manadgement of the multigrid cycles are crucial points to get stable and fast convergences and to save CPU time. Concerning the coupling periods, a good choice is: $cp_0 = 15$, $cp_1 = 60$ and $cp_2 = 120$ (if any).

NOMENCLATURE

- cp_l : coupling period for grid Ω_l
- cp_l^0 : first coupling period for grid Ω_l
- $\overrightarrow{G}$: mixture mass flux (= $\rho\,\overrightarrow{v}$)
- $\overrightarrow{g}$: gravity (m s^{-2})
- H : mixture specific enthalpy (J kg^{-1})
- H_{ls} : saturated liquid specific enthalpy (J kg^{-1})
- l_{max} : maximal number of computational grids

- L : latent heat (J kg^{-1})
- L_v : typical vortex length (m)
- m : multigrid cycle counter
- n : iteration (or pseudo-time step) counter
- P : pressure (Pa)
- P_l^k : grid Ω_k to grid Ω_l transfer operator
- Q : heat source (W m^{-3})
- S_l: Coarse grid (Ω_l) balance equation RHS (FAS)
- t : time (s)
- $\overrightarrow{v}$: mixture velocity (m s^{-1})
- $\overrightarrow{v_R}$: relative velocity (gas minus liquid, m s^{-1})
- x : static quality ($\equiv \frac{H-H_{ls}}{L}$)
- α : multigrid relaxation parameter
- β : porosity ($:= \omega_m/\omega$)
- δt : Pseudo-time step (s)
- χ_T : turbulent diffusion coefficient for the mixture energy equation (kg m^{-1} s^{-1})
- μ_T : two-phase turbulent dynamic viscosity (kg m^{-1} s^{-1})
- ρ : mixture density (kg m^{-3})
- $\bar{\Lambda}$: two-phase friction tensor (s^{-1})
- ω : volume of the homogenization cell (m^3)
- ω_m : mixture volume of the homogenization cell (m^3)
- Ω_l : computation domain grids ($0 \leq l \leq l_{max}$)
- ϕ^i : nodal function
- ψ^e : element function

REFERENCE

M. Belliard. Multigrid preconditionning in the genepi software. Technical Report DTP/STH/LMTA/2001/04, CEA, Cadarache, France, 2001.

M. Belliard. Multigrid preconditioning of the steam generator two-phase mixture balance equations. *submitted to Progress in Comp. Fluid Dyn.*, 2003.

J.L. Campan and J.C. Bouchter. Steam generator experiment for advanced computer code qualification : CLOTAIRE international program. In *Third International Topical Meeting on nuclear power plant thermohydraulics and operations*, Seoul, April 1988.

M. Grandotto and P. Obry. Calculs des écoulements diphasiques dans les échangeurs par une méthode aux éléments finis. *Revue Européenne des Eléments Finis*, 5(1):53–74, 1996.

P.M. Gresho and S.J. Chan. On the theory of semi implicit projection methods for viscous incompressible flow and its implementation via finite element method that also introduces a nearly consistent matrix. i, theory. *International Journal for Numerical Methods in Fluids*, 11(5):587–620, 1990.

P. Obry, J.L. Cheissoux, M. Grandotto, J.P. Gaillard, E. De Langre, and M. Bernard. An advanced steam generators design 3D code. In *ASME Winter Annual Meeting*, Dallas, Texas, USA, November 1990.